Available online at www.sciencedirect.com

SCIENCE DIRECT

Diamond & Related Materials 14 (2005) 1270–1276

DIAMOND AND RELATED MATERIALS

www.elsevier.com/locate/diamond

Characterization of the mechanical properties of diamond-like carbon films

Sung-Jin Cho[1], Jin-Won Chung[2], Kwang-Ryeol Lee*

Future Technology Research Division, Korea Institute of Science and Technology, P. O. Box 131, Cheongryang, Seoul, 130-650, Republic of Korea

Available online 25 February 2005

Abstract

A recently suggested method to measure the elastic modulus of diamond-like carbon (DLC) films was reviewed. This method used a DLC bridge or free overhang which is free from the mechanical constraint of the substrate. Because of the high residual compressive stress of the DLC film, the bridge or the overhang exhibited a sinusoidal displacement on removing the mechanical constraint. Measuring the amplitude and wavelength of the sinusoidal displacement made it possible to measure the strain of the film which occurred by stress relaxation. Combined with independent stress measurement using the laser reflection method, this method allowed the calculation of the biaxial elastic modulus of the DLC film. This method was successfully applied to obtain the elastic properties of various DLC films from polymeric hydrogenated amorphous carbon (a-C:H) to hard tetrahedral amorphous carbon (ta-C) films. Since the substrate is completely removed from the measurement system, this method is insensitive to the mechanical properties of substrate. The mechanical properties of very thin DLC films could be thus measured and then can reveal the structural evolution of a-C:H films during the initial stages of deposition.

Keywords: Diamond-like carbon; Residual compressive stress; Elastic modulus; Structural evolution

1. Introduction

The excellent mechanical properties of diamond-like carbon (DLC) film such as high hardness, high wear resistance, low friction coefficient and high ratio of elastic modulus to the density have motivated studies into various applications. Among the applications are protective coatings for various tools and over coats for hard disks, speaker diaphragms or surface acoustic wave devices [1–3]. For these applications, it would be essential to measure the elastic properties of DLC films as well as the hardness. The elastic properties are also critical for applications to micro-electromechanical systems (MEMS).

Generally, the mechanical properties of thin films are different from that of the bulk materials due to defects or textures in the thin films. Furthermore, the properties of DLC films can be varied over a wide range by changing the deposition condition [1]. It is thus necessary to measure the properties of as-deposited DLC films. Many methods have been suggested to measure the mechanical properties of thin films. Nanoindentation is the most widely used method to measure the hardness and elastic modulus of thin films [4]. However, the difficulties of nanoindentation for thin films arise from high sensitivity to the substrate, especially when applying to a system which has a large difference in mechanical properties between substrate and the film. The substrate effect is more significant in measuring the elastic modulus than in measuring hardness. Because elastic strain field is much wider than the plastic strain field, the elastic behavior during unloading in nanoindentation measurement is dominated by the elastic properties of the substrate. The effect of a truncated indentation tip should also be considered for the analysis of shallow indentation for thin

* Corresponding author. Tel. : +82 2 958 5494; fax: +82 2 958 5509.
E-mail address: krlee@kist.re.kr (K.-R. Lee).
[1] Presently at PaiChai High School, Seoul, Korea.
[2] Presently at Devices and Materials Lab., LG Electronics Institute of Technology, Seoul, Korea.

0925-9635/$ - see front matter © 2004 Elsevier B.V. All rights reserved.
doi:10.1016/j.diamond.2004.11.034

films [5]. Other methods using the propagation behavior of long wavelength acoustic phonons are also employed for elastic modulus measurement [6–8]. However, these methods need sophisticated instrumental and analysis techniques to be applied for very thin films. These methods also need density of the film that is generally dependent on the atomic bond structure and thus the deposition condition. Precise measurement of the mechanical properties of very thin films remains as a challenging problem.

Recently, a simple method to measure the elastic properties of the DLC films deposited on Si wafer was suggested [9–12]. Typical DLC films have high residual compressive stress up to 10 GPa [1]. The residual stress has been considered as the main reason for instability of the coating, since the film buckles when the adhesion of the film is not sufficient to suppress the interfacial delamination. However, this phenomenon can be used to measure the elastic properties. When the thickness of the film is much smaller than that of the substrate, the residual stress of DLC film can be measured independently of the elastic modulus of thin film from the curvature of the film/substrate composite [13]. If one can measure the strain of the film required to adhere on the substrate, biaxial elastic modulus would be thus obtained from a simple stress–strain relation of isotropic thin films.

Two methods were suggested to measure the strain of DLC films during the residual stress relaxation [9,10]. The method involved producing DLC bridges between DLC patches using a conventional lithography technique or etching a side of Si substrate using the DLC film as an etching mask. Because the bridges were free from the mechanical constraint of the substrate, the shape of the bridge appeared with a sine wave of one wavelength which is equal to the bridge length. Etching a Si substrate method resulted in unstressed DLC free overhang sinusoidal in shape. It was possible to obtain the strain by measuring the amplitude and the wavelength of the sinusoidal deflection of the bridge or the overhang.

In this paper, we reviewed the details of experimental procedure for preparing the stress relaxed bridge or overhang and theoretical analysis of the relaxed microstructure to calculate the biaxial elastic modulus of DLC film. Application results of the present method are also summarized. It is worth noting that the elastic modulus measured by this method is not affected by the mechanical properties of substrate, because the substrate is completely excluded from the measurement process. The elastic properties of extremely thin DLC film could thus be measured by these methods, which revealed the structural evolution behavior of the DLC film during the initial stage of deposition. This phenomenon would be important for the industrial application of DLC films of thickness much smaller than 1 μm. For example, protective layers for hard disk of large storage capacity should be less than 5 nm due to the reduced magnetic spacing between the magnetic layer and the read/write head [14]. The mechanical property and atomic bond structure of the thin protective layer is one of the major concerns in the increased development of hard disks.

2. Experimental procedure

DLC bridges were prepared using a conventional lithography. DLC films were deposited on a SiO_2 sacrificial layer of 0.5 μm thick which was grown on Si (100) wafer by thermal oxidation. The DLC films were patterned to obtain thin DLC bridges between 100 μm×327 μm DLC patches. Photoresist was spin coated on the DLC films and developed using the mask pattern of Fig. 1. The bridge length and width were varied from 60 to 150 μm and from 12 to 15 μm, respectively. The exposed DLC film was etched using an oxygen plasma and the sacrificial SiO_2 layer was then removed by a buffered oxide etcher (BOE). Fig. 2(a) shows a typical microstructure of the DLC bridges obtained by the present method. Since the DLC patch is much larger than the width of the bridges, etching the SiO_2 sacrificial layer could relieve the residual stress of only the DLC bridges by separating the bridge from the substrate. The length of the bridge was recovered to its unstressed one, while the ends were fixed by the DLC patches. The center of the bridges was thus deformed upward resulting in a sinusoidal shape.

DLC free overhang can be prepared by a simple substrate etching technique. DLC films were deposited on Si (100) wafers. The DLC coated Si wafers were cleaved along the <011> direction. The Si substrates for the samples were etched in dilute KOH solution (5.6 mol/l) at 70 °C for 1–120 min. In order to obtain uniform etching, the solution was agitated during the etching process. Because of anisotropy etching rate of Si in KOH solution, the <011> direction of the {111} plane was maintained as an etching front. However, DLC films were not damaged due to their chemical inertness. Fig. 2(b) shows the typical microstructure of the free overhang. Because the mechanical constraint of the substrate was removed by the etching process, the length of the free overhanging edge was recovered to its unstressed one resulting in periodic sinus-

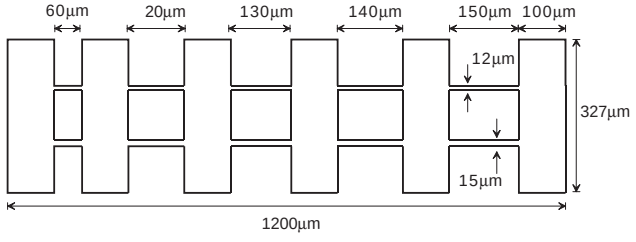

Fig. 1. Schematic of the bridge pattern.

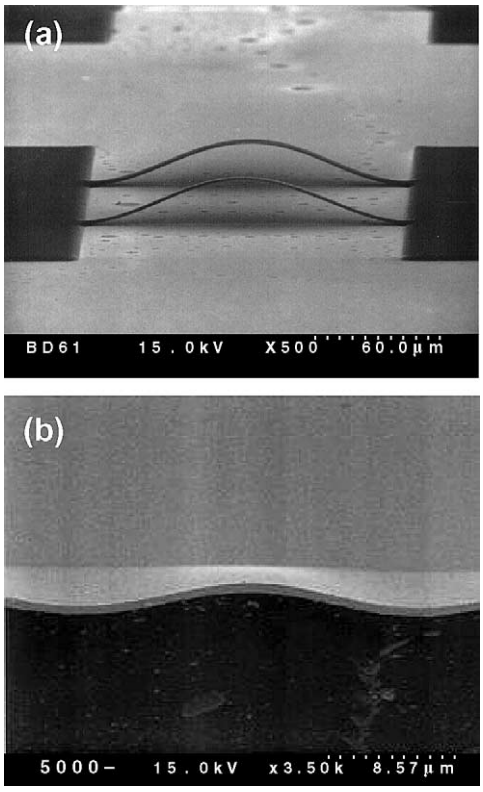

Fig. 2. Typical morphology of DLC bridges (a) and free overhang (b). The film was deposited by r.f. PACVD at a bias voltage of −100 V for DLC bridge and −400 V for overhang and a deposition pressure 1.33 Pa.

oidal deformation. The amplitude and the wavelength of the sinusoidal deformation were determined by end-on-view of scanning electron microscopy (SEM).

3. Theoretical analysis

Because of the analogy with the mechanical situation between the free overhang and the bridge, a theoretical analysis of the bridge can be applied to both cases. Fig. 3 shows the schematic of the buckled thin film with the pads at either end. If the aspect ratio of the bridge length to the width is sufficiently large, the shape of the relieved bridge would be described by one-dimensional buckling phenomena. Most of the residual stress, σ_o, was relieved by removing the mechanical constraint of the substrate. However, the buckled film was balanced by the remaining stress in the film which is approximately equal to the critical stress of buckling, σ_c, as shown by Evans and Hutchinson in a buckled wide column [15]. In the case of elastically isotropic thin films, the relieved stress, $\sigma_o - \sigma_c$, is thus given by product of the biaxial elastic modulus, $E/(1-v)$ and the strain of the buckling, ε_x;

$$\Delta\sigma = \sigma_o - \sigma_c = \frac{E}{1-v}\varepsilon_x. \tag{1}$$

In most experimental conditions where the film thickness was much smaller than the maximum deflection of the bridge, the critical stress is much smaller than the residual compressive stress [10]. Hence, Eq. (1) can be simplified as

$$\Delta\sigma = \frac{E}{1-v}\varepsilon_x \approx \sigma_o \tag{2}$$

From the momentum balance condition, the governing equation for buckling is given by [16];

$$D\frac{\partial^4 W}{\partial x^4} + \sigma_c t\frac{\partial^2 W}{\partial x^2} = 0, \tag{3}$$

where D is the flexural rigidity, $Et^3/12(1-v^2)$, W the displacement of the film in the z-direction and t the film thickness. By solving Eq. (2) with the following boundary conditions:

$$\text{at } x = -\frac{\lambda}{2}, \quad W = \frac{\partial W}{\partial x} = 0 \tag{4}$$

$$\text{at } x = \frac{\lambda}{2}, \quad W = \frac{\partial W}{\partial x} = 0, \tag{5}$$

one can obtain the shape of the buckled film and the critical stress as follows:

$$W(x) = A_o\left\{1 + \cos\left(\frac{2\pi}{\lambda}x\right)\right\}, \tag{6}$$

$$\sigma_c = \frac{4\pi^2 D}{\lambda^2 t}. \tag{7}$$

The strain of the bridge can be expressed by averaging the local strain over the bridge length:

$$\varepsilon_x = \frac{1}{\lambda}\int_{-\lambda/2}^{\lambda/2}\frac{1}{2}\left(\frac{\partial W}{\partial x}\right)^2 dx \tag{8}$$

$$= \frac{1}{\lambda}\int_{-\lambda/2}^{\lambda/2}\left(\frac{2\pi A_o}{\lambda}\right)\sin^2\left(\frac{2\pi}{\lambda}x\right)dx \tag{9}$$

$$= \left(\frac{\pi A_o}{\lambda}\right)^2. \tag{10}$$

From Eqs. (2) and (10), the biaxial elastic modulus can be expressed as:

$$\frac{E}{1-v} \approx \left(\frac{\lambda}{\pi A_o}\right)^2 \sigma_o. \tag{11}$$

Eq. (11) shows that the biaxial elastic modulus can be obtained by measuring the amplitude with known values of the bridge length and the residual compressive stress.

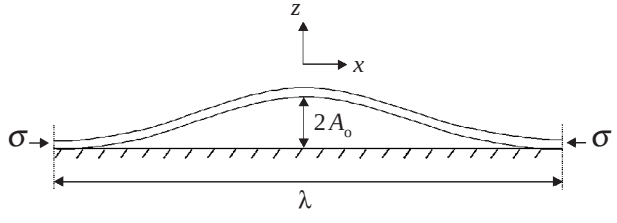

Fig. 3. Schematic of the buckled thin film.

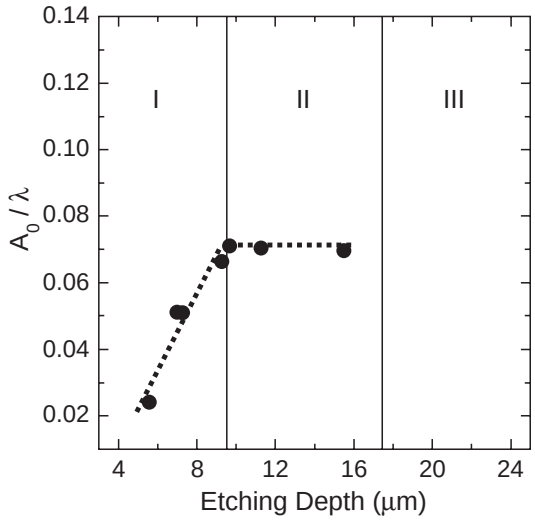

Fig. 4. Typical values of A_o/λ for various etching depths. The data were obtained with a film of thickness 546 nm deposited by r.f. PACVD at the negative bias voltage of −400 V and a deposition pressure 1.33 Pa [11].

For thin films where the film thickness is much smaller than that of substrate, the residual stress can be determined independently of the mechanical properties of thin film. The length of the bridge is predetermined by the lithographic pattern of Fig. 1. In the case of the free overhang, however, there is no constraint to determine the wavelength of the sinusoidal displacement. The biaxial elastic modulus is obtained by measuring both the amplitude and the wavelength of the free overhang for a film with known residual compressive stress. However, it must be noted that its etching depth for the free overhang should be optimized so that the stress at the end of the overhang is sufficiently relaxed from the constraint of the substrate [11]. Fig. 4 exhibits the typical change in A_o/λ values with etching depth. The data were obtained with a-C:H film of thickness 546 nm. The behavior can be divided into three regions as indicated in Fig. 4. In region I (small etching depth), the sinusoidal free overhang is not well developed due to insufficient stress relaxation. However, in region III (large etching depth), a continuous and periodic sinusoidal free overhang could not be maintained due to collapse of the large free overhang. The values of A_o/λ in these regions are, thus, meaningless for the elastic modulus calculation. In region II, a continuous periodic sinusoidal free overhang could be observed resulting in a fixed value of A_o/λ regardless of etching depth. The value in region II should be selected for elastic modulus calculation.

4. Experimental results and discussion

Table 1 summarized the elastic moduli of DLC film using the bridge and the free overhang methods. For comparison, plane strain moduli measured by nanoindentation, and Young's moduli measured by acoustic wave velocity measurement are also included. The measured films are hydrogenated amorphous carbon (a-C:H) films of thickness 1.3±0.1 μm deposited by radio frequency plasma assisted CVD using benzene as precursor. The deposition pressure was fixed at 1.33 Pa. At the deposition conditions, the structure of the DLC films changed from polymer-like to diamond-like one with increasing negative bias voltage from −100 to −550 V [17]. The hardness of the films measured by nanoindentation increased from 2.3 to 15.4 GPa with an increasing negative bias voltage.

Table 1 shows that both methods using the DLC bridge and free overhang resulted in the same values of the biaxial elastic moduli within the error range. The elastic modulus increases from about 11 to 155 GPa with negative bias voltage, which is consistent with the structural change in this bias voltage range. It was confirmed that the measured values are not dependent on the bridge length in the range from 60 to 150 μm and film thickness from 0.5 to 1.5 μm [9,10]. The biaxial elastic moduli are comparable to those measured by nanoindentation and acoustic wave velocity measurement, if the Poisson's ratio of the DLC film is assumed to be 0.3. Although the values exhibit some difference in soft polymeric films (those of low negative bias voltages), it should be considered that the effect of the mechanical properties of the substrate can be more significant with increasing difference in the mechanical properties between the film and the substrate. It can be thus said that reasonable values of the elastic modulus are obtained by the present methods.

The major advantages of these methods are revealed when studying the mechanical properties of very thin DLC films. The free overhang method was applied to measure the elastic properties of a-C:H and tetrahedral amorphous carbon (ta-C) films over the thickness range from 33 nm to 1.1 μm [11,12]. a-C:H film was deposited by r.f. PACVD using benzene at a negative bias voltage of −400 V and a deposition pressure 1.33 Pa. The ta-C films were deposited by filtered vacuum arc using a graphite target at a substrate bias of −50 V and a deposition pressure 7×10^{-3} Pa. Fig. 5 summarizes the biaxial elastic moduli of a-C:H films of various film thicknesses. In order to investigate the substrate effect, the films were deposited on Si, SiO_2 and W

Table 1
Elastic moduli of a-C:H film deposited by r.f. PACVD for various negative bias voltages

Bias voltage (V)	$E/(1-\nu)$		$E/(1-\nu)^2$	E
	Bridge	Overhang	Nanoindentation	Acoustic wave velocity
−100	11.0±0.5	11.0±1.0	20.9±4.3	
−250	59.3±10.1	57.1±7.5	75.7±6.7	65.6±1.9
−400	117.6±7.3	118.9±11.3	99.1±2.8	99.1±2.2
−550	154.7±12.0	161.5±15.0	138.5±11.0	128.4±2.4

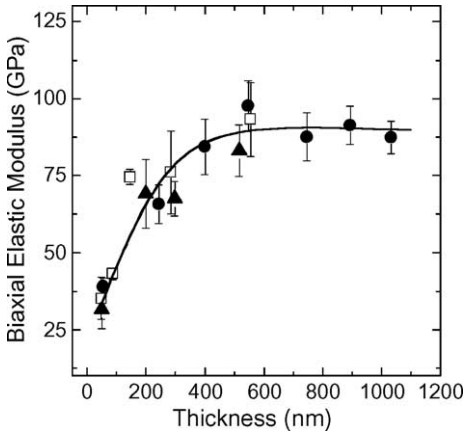

Fig. 5. Calculated biaxial elastic moduli of a-C:H films for various film thicknesses and substrate materials [11].

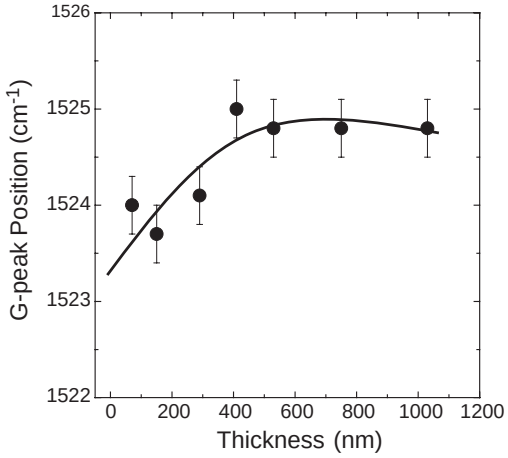

Fig. 6. Dependence of the G-peak position of Raman spectroscopy on the a-C:H film thickness after residual stress effect on the G-peak position was corrected.

substrates. Regardless of the substrate materials, the elastic moduli increased with increasing film thickness and saturated when the film thickness was larger than 500 nm. The saturated value is comparable to the plane strain modulus of 75±5 GPa that was obtained by nanoindentation with the same film of thickness larger than 1 μm. If the Poisson's ratio is assumed to be 0.3, the elastic modulus, E, can be estimated to be 66±4 GPa in both cases.

When the film was thinner than 500 nm, the elastic modulus of the a-C:H film monotonically decreased to 35 GPa as the film thickness decreased. Because the substrate is not involved in this measurement, this decreasing behavior is not due to the effects of the substrate. The effect of the interfacial reaction layer can be significant with decreasing film thickness. However, Fig. 5 shows a similar behavior for the elastic modulus with film thickness regardless of the substrate materials, which also excludes the effect of the interfacial reaction layer. The most possible reason for the decreasing elastic modulus of the very thin films would be the evolution of the film structure during the early stages of growth. The structural change during film growth has been observed via the Raman spectra obtained for various film thicknesses. The Raman spectrum analysis for DLC films includes deconvolution of the spectrum using two Gaussian peaks; the G- and D-peak [18]. It is empirically known that the G-peak position illustrates the changes in atomic bond structure of the film. Fig. 6 shows the G-peak position for various film thicknesses. It is interesting to note that the G-peak position shows the same dependence on film thickness as the elastic modulus: when the film thickness is less than 500 nm, the G-peak monotonically shifted to a lower wave number (it has been reported that the G-peak position shifts upward by 4.1 cm^{-1} per GPa of residual compressive stress [19]; the data in Fig. 6 were the corrected values to exclude the effect of the residual stress). This result shows that the decrease in elastic modulus of very thin film is related to the structural changes in the film.

In contrast to the trend in a-C:H films, a decrease in the elastic modulus of very thin films was not observed in ta-C film. Fig. 7 shows the biaxial elastic moduli of ta-C films for various film thicknesses. A constant value of 600±50 GPa was obtained in this range of film thickness considered. When the film thickness was less than 100 nm, the elastic modulus in fact increased slightly. The results of Figs. 5 and 7 show that ta-C film is superior to a-C:H film for the applications of very thin films, and that the structural evolution during the early stages of growth is strongly dependent on the deposition process.

The free overhang method was employed for a more systematic study on the structural evolution of a-C:H films deposited by r.f. PACVD [12]. The films were deposited at various cathode bias voltages and deposition pressures using methane as the precursor gas. Lee et al. reported the precursor gas effect on the structure of the DLC film under similar deposition conditions [17]. The films deposited from methane exhibited growth behavior depending on the ion energy; as the ion energy increased, the deposited film changed from polymeric amorphous carbon to a dense diamond-like film,

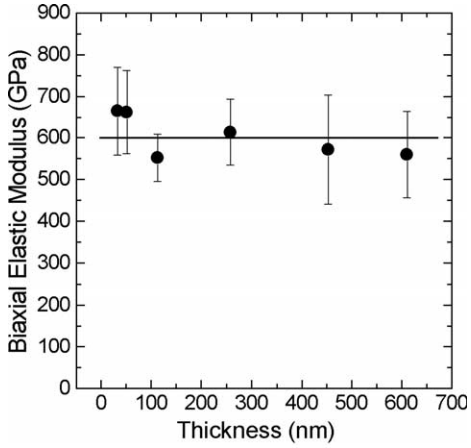

Fig. 7. Calculated biaxial elastic moduli of ta-C films for various film thicknesses [11].

and then to a graphitic type. Hence, DLC films with a wide range of physical properties could be investigated.

In the r.f. PACVD process, the ion energy depends on both the time averaged cathode sheath potential by which the ion is accelerated to the growth surface, and inelastic collisions between ions and neutrals in the sheath. The latter is dependent on deposition pressure, and the former is approximately the same as the negative bias voltage of the cathode in a strongly asymmetric r.f. discharge system. For a precursor gas, the mean ion energy is thus known to be proportional to $V_b/\sqrt{P}$, where V_b is the bias voltage on the cathode and P is the deposition pressure [20]. The residual compressive stress and hardness of the film show maxima of 2.2 GPa and 19.5 GPa respectively, at a value of $V_b/\sqrt{P}$ of approximately 100 V/m Torr$^{1/2}$.

Fig. 8(a) shows the dependence of the biaxial elastic modulus on the film thickness for various values of $V_b/\sqrt{P}$. The numbers on the data are the values of $V_b/\sqrt{P}$ in units of V/m Torr$^{1/2}$. When the value of $V_b/\sqrt{P}$ was 20 V/m Torr$^{1/2}$, the biaxial elastic modulus increased from 35 to 50 GPa with increasing film thickness from 50 to 300 nm. However, at the optimum value of $V_b/\sqrt{P}$=100 V/m Torr$^{1/2}$ where the deposited film has the maximum hardness and residual compressive stress, the effect of the film thickness on the biaxial elastic modulus was much reduced. In the present range of film thickness from 50 to 330 nm, the biaxial elastic modulus of approximately 120 GPa was obtained regardless of film thickness. On the other hand, when the value of $V_b/\sqrt{P}$ is larger than 100 V/m Torr$^{1/2}$, the biaxial elastic modulus significantly decreased with decreasing film thickness. When the value of $V_b/\sqrt{P}$ was 166 V/m Torr$^{1/2}$, the biaxial elastic modulus decreased from 108 to 74 GPa as the film thickness decreased from 420 to 50 nm. Similarly, at a value of $V_b/\sqrt{P}$ *of* 233 V/m Torr$^{1/2}$, the biaxial elastic modulus varied from 69 to 30 GPa over the same thickness range.

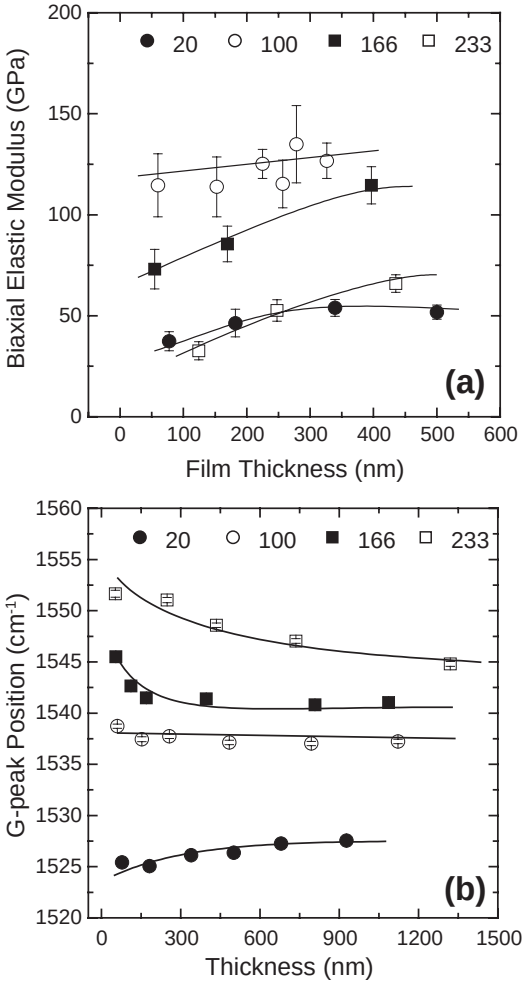

Fig. 8. (a) Dependence of the biaxial elastic modulus on the film thickness for various values of $V_b/\sqrt{P}$. Numbers in annotate are the values of $V_b/\sqrt{P}$ in units of V/m Torr$^{1/2}$. (b) Dependence of the G-peak position of Raman spectra on film thickness for various values of $V_b/\sqrt{P}$. Numbers in annotate are the values of $V_b/\sqrt{P}$ in units of V/m Torr$^{1/2}$.

Fig. 8(b) shows the dependence of the G-peak position of the Raman spectra on film thickness for various values of $V_b/\sqrt{P}$. At the optimum ion energy ($V_b/\sqrt{P}$=100 V/m Torr$^{1/2}$), the G-peak position did not vary with film thickness. This behavior can be compared with the constant biaxial elastic modulus regardless of film thickness (see Fig. 8 (a)). This result shows that at the optimum ion energy, the structure of the initial deposition layer is identical to that obtained at the later deposition stage. On the other hand, when the value of $V_b/\sqrt{P}$ was smaller than the optimum value, the G-peak position shifted to a lower wave number with decreasing film thickness. Because the polymeric component shifted the G-peak to a lower wave number, it can be said that the initial deposition layer has higher polymeric content. When the value of $V_b/\sqrt{P}$ was larger than 100 V/m Torr$^{1/2}$, however, an upward G-peak shift was observed for thin films, which shows that a greater graphitic component was involved in the initial deposition layer.

The present results show that the structural evolution occurs when the ion energy used in the film deposition deviates from the optimum value for the dense and hard a-C:H film deposition. In these cases, the elastic modulus of the very thin film was smaller than that obtained in the thick film. However, the reason for the decrease in the elastic modulus was different according to the deposition condition. When the ion energy was smaller than the optimum value where the polymeric film was obtained, the initial deposition layer contained more polymeric component. In the opposite case where ion energy was higher than the optimum value, the initial deposition layer contained a greater graphitic component.

5. Conclusions

A recently suggested method for the measurement of thin film elastic modulus has been reviewed. The most significant result of the present work is to show that the mechanical properties of the diamond-like carbon film can be characterized from the stress relaxation behavior by

eliminating the mechanical constraint of the substrate. This method results in a simple and accurate analysis, since no external force is applied to the film/substrate system. It was successful to apply the method to measure the elastic properties of various DLC films from polymeric a-C:H films deposited by r.f. PACVD to very hard ta-C films deposited by the filtered vacuum arc process. Furthermore, this method can provide a tool to characterize the mechanical properties of very thin films. In contrast to other measuring methods, the present method is not sensitive to the mechanical properties of the substrate because the substrate is removed to measure the strain. Characterization of the mechanical properties of very thin film revealed the structural evolution during initial stages of deposition. While ta-C films deposited by filtered vacuum arc process exhibit a homogeneous structure and uniform mechanical properties through the film thickness, a-C:H films deposited by r.f. PACVD exhibit a structural evolution during initial stages of deposition. The structural evolution in a-C:H can be minimized when using an optimum deposition condition where hard and dense film can be obtained.

Acknowledgement

This research was supported by a grant (code 04K1501-01110) from 'Center for Nanostructured Materials Technology' under 'the 21st Century Frontier R&D Programs' of the Ministry of Science and Technology of Korea and J&L Tech. Co. Ltd.

References

[1] J. Robertson, Mater. Sci. Eng., R 37 (2002) 129.
[2] N. Fujimori, New Diam. 3 (1989) 20.
[3] T. Imai, H. Nakahara, N. Fujimori, US patent 4,952,832 (1990).
[4] W.C. Olver, G.M. Pharr, J. Mater. Res. 7 (1992) 1564.
[5] T. Sawa, Y. Akiyama, A. Shinmamoto, K. Tanaka, J. Mater. Res. 14 (1999) 2228.
[6] P. Pastorelli, A.C. Ferrari, M.G. Beghi, C.E. Bottani, J. Robertson, Diamond Relat. Mater. 9 (2000) 825.
[7] Y. Kim, J. Electron. Mater. 26 (1997) 1002.
[8] D. Scheider, Th. Witke, Th. Schwarz, B. Schöneich, B. Schultrich, Surf. Coat. Technol. 126 (2000) 136.
[9] S.-J. Cho, K.-R. Lee, K.Y. Eun, J.H. Hahn, D.-H. Ko, Thin Solid Films 341 (1999) 207.
[10] S.-J. Cho, K.-R. Lee, K.Y. Eun, J.-H. Jeong, D. Kwon, Diamond Relat. Mater. 8 (1999) 1067.
[11] J.-W. Chung, C.-S. Lee, D.-H. Ko, J.H. Hahn, K.Y. Eun, K.-R. Lee, Diamond Relat. Mater. 10 (2001) 2069.
[12] J.-W. Chung, D.-H. Ko, K.Y. Eun, K.-R. Lee, Diamond Relat. Mater. 11 (2002) 1441.
[13] K.-R. Lee, Y.-J. Baik, K.Y. Eun, MRS Proc. 308 (1993) 101.
[14] B. Cord, J. Scherer, IEEE Trans. Magn. 36 (2000) 67.
[15] A.G. Evans, J.W. Hutchinson, Int. J. Solids Struct. 20 (1983) 455.
[16] S. Timoshenko, J. Gere, Theory of elastic stability, 2nd ed., McGraw-Hill, New York, 1961.
[17] K.-R. Lee, Y.-J. Baik, K.Y. Eun, Diamond Relat. Mater. 3 (1994) 1230.
[18] M. Yoshigawa, G. Katagiri, H. Ishida, T. Akamatsu, J. Appl. Phys. 64 (1988) 6464.
[19] J.K. Shin, C.S. Lee, K.-R. Lee, K.Y. Eun, Appl. Phys. Lett. 27 (2001) 631.
[20] A. Bubenzer, B. Dischler, G. Brandt, P. Koidl, J. Appl. Phys. 54 (1993) 4590.